Journal of Power Sources 185 (2008) 1594–1597

Contents lists available at ScienceDirect

Journal of Power Sources

journal homepage: www.elsevier.com/locate/jpowsour

Short communication

Anodic deposition of porous vanadium oxide network with high power characteristics for pseudocapacitors

Chi-Chang Hu[a,*], Chao-Ming Huang[b], Kuo-Hsin Chang[a,b]

[a] Department of Chemical Engineering, National Tsing Hua University, Hsin-Chu 30013, Taiwan
[b] Department of Chemical Engineering, National Chung Cheng University, Chia-Yi 621, Taiwan

ARTICLE INFO

Article history:
Received 18 June 2008
Received in revised form 8 August 2008
Accepted 12 August 2008
Available online 19 August 2008

Keywords:
Vanadium oxide
3-D network
Anodic deposition
Pseudocapacitors
H_2O_2

ABSTRACT

A new type vanadium oxide deposit with a porous, three-dimensional (3-D) network architecture plated at 0.7 V (vs. Ag/AgCl) from 25 mM $VOSO_4$ with 5 mM H_2O_2 shows capacitive-like behavior at 250 mV s^{-1} and $C_S \approx 167$ F g^{-1} at 25 mV s^{-1} in 3 M KCl for pseudocapacitor applications. This work also emphasizes that anodic deposition of vanadium oxide does occur at a potential much more negative to oxygen evolution from aqueous $VOSO_4$ solutions due to the presence of V^{5+} by adding H_2O_2. Through the X-ray photoelectron spectroscopic analyses, this oxide deposit, mainly consisting of V^{5+} with 11 mol.% V^{4+}, shows a hydrous nature. The unique power characteristics of this hydrous vanadium oxide are reasonably attributed to its intrinsic porous and crystalline structure produced by means of this novel anodic deposition process at a potential much more negative to the oxygen evolution reaction.

1. Introduction

Vanadium oxides in various forms (e.g., $H_2V_3O_8$, V_2O_5) are widely studied as an electrode material for Li-ion batteries (LIBs) [1–6] and electrochemical capacitors (ECs) in organic electrolytes [7–9]. Since several vanadium oxides with layered structures show the redox intercalation ability for various cations [5,6], these materials are considered as an important electrode material in developing high energy density LIBs [6] and high power ECs [10,11].

Many chemical routes, such as hydrothermal synthesis [12], sol–gel method [13], and electrochemical deposition [1], were developed to prepare vanadium oxides. Among these methods, electrochemical deposition is considered as a simple, one-step, and cost-effective technique. The structure, morphology, and uniformity of oxides can be controlled by adjusting the plating parameters such as deposition mode, applied potential, current density, bath temperature, concentration of precursors, and addition of complex/additive agents [14,15]. In addition, preparation of vanadium oxides through anodic deposition from aqueous $VOSO_4$ solutions has been considered as an effective method [1,16] which was developed by Sato et al. [17,18]. Anodic deposition of V_2O_5, however, was found to occur in two steps involving oxygen evolution at highly positive potentials [19,20]. Moreover, the deposition current density observed in the negative scan of CV was found to be much larger than that in its corresponding positive scan [16]. Furthermore, chemical analyses revealed that the obtained compounds are hydrated, mixed valence compounds containing V^{4+} and V^{5+} [16]. These facts indicate the very complicated deposition mechanism of vanadium oxides in the oxygen evolution region.

In our previous study [12], a designed precursor solution containing V^{5+} and V^{4+} effectively promotes the formation rate of $H_2V_3O_8$ single-crystal nanobelts under hydrothermal conditions, indicating the importance of V^{5+}/V^{4+} ratios in the precursor solution. The finding provides the idea that anodic deposition of vanadium oxide is probably influenced by the presence of V^{5+} species in the precursor solution. This work demonstrates the success in depositing a new type vanadium oxide at potentials much more negative to oxygen evolution from aqueous $VOSO_4$ solutions with certain amount of V^{5+} species (i.e., 25 mM $VOSO_4$ with 5 mM H_2O_2). This novel oxide deposit showing a porous three-dimensional (3-D) network architecture possesses high power characteristics (capacitive-like behavior at 250 mV s^{-1}) and acceptable specific capacitance ($C_S \approx 167$ F g^{-1} at 25 mV s^{-1}) for pseudocapacitor applications.

2. Experimental

Hydrous vanadium oxide (denoted as $VO_x{\cdot}yH_2O$) was directly electrodeposited onto graphite substrates under a potentiostatic mode. The pretreatment procedure of 10 mm × 10 mm × 3 mm

* Corresponding author. Tel.: +886 3 573 6027; fax: +886 3 573 6027.
E-mail address: cchu@che.nthu.edu.tw (C.-C. Hu).

0378-7753/$ – see front matter © 2008 Elsevier B.V. All rights reserved.
doi:10.1016/j.jpowsour.2008.08.017

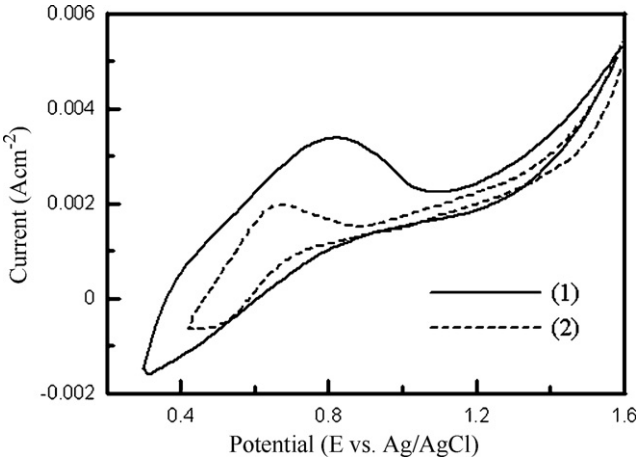

Fig. 1. Cyclic voltammograms measured at 20 mV s^{-1}: (1) in 25 mM $VOSO_4$ and (2) with the addition of 5 mM H_2O_2 at 25 °C.

graphite substrates completely followed our previous work [10,14]. These substrates were carefully coated with a thick film of PTFE with an exposed surface area of 1 cm^2 and $VO_x{\cdot}yH_2O$ was electroplated at 0.7 V vs. Ag/AgCl from a 25 mM $VOSO_4$ with 5 mM H_2O_2 at 25 °C. The weight of a typical $VO_x{\cdot}yH_2O$ film is ca. 2.0 ± 0.1 mg cm^{-2}, which can be controlled by varying the passed charge. After cleaning and drying, the $VO_x{\cdot}yH_2O$/G electrode was characterized by electrochemical and textural analyses.

The morphology of $VO_x{\cdot}yH_2O$ was observed using a field emission scanning electron microscope (FE-SEM, Hitachi S4800 type I). The chemical environments of $VO_x{\cdot}yH_2O$ were obtained from the X-ray photoelectron spectra (XPS) measured by an XPS spectrometer (Kratos Axis Ultra DLD), employed Al monochro-

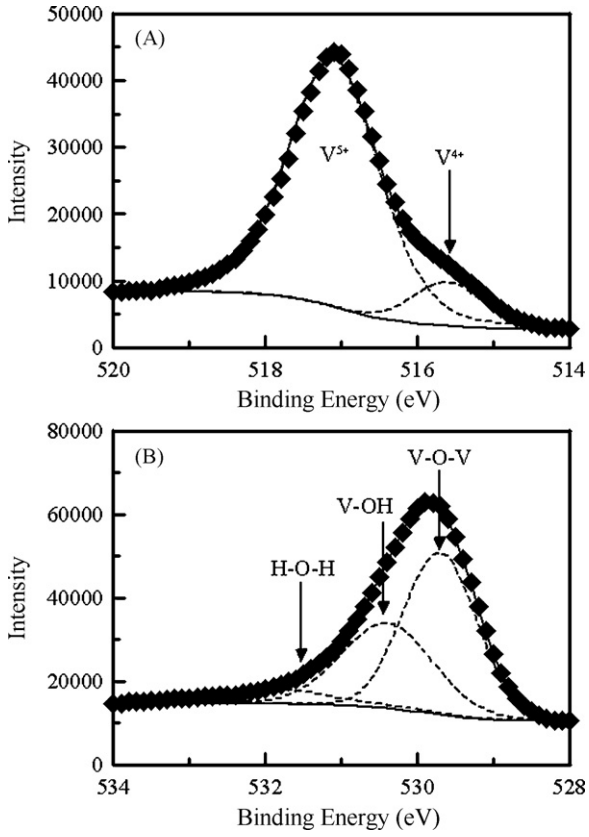

Fig. 2. XPS core-level spectra of (A) V $2p_{3/2}$ and (B) O 1s for a $VO_x{\cdot}yH_2O$ deposit. The dot, dashed, and solid lines are the experiment, fitting, and resultant spectra, respectively.

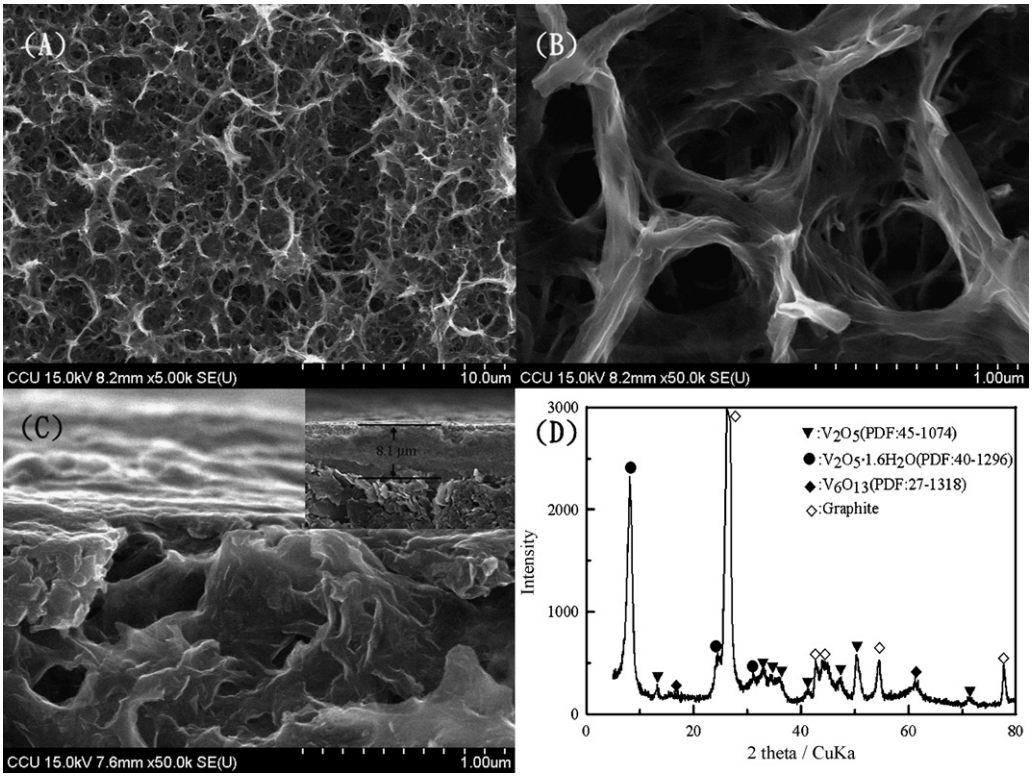

Fig. 3. (A and B) Top and (C) cross-section SEM images of a $VO_x{\cdot}yH_2O$ deposit under (A) low and (B) high magnifications; (D) the corresponding XRD pattern; inset of 3(C) indicates an average thickness of 8.1 μm.

mator ($h\nu$ = 1486.69 eV) irradiation as the photosource. The X-ray diffraction (XRD) pattern was obtained with a glancing-angle X-ray diffractometer (Rigaku D/MAX2500) using a Cu target (Cu K_α = 1.5418 Å) at an angular speed of 1° (2θ) min^{-1}. Electrochemical characteristics of $VO_x{\cdot}yH_2O$ were examined by means of an electrochemical analyzer system, CHI 633A (CH Instruments, USA) in a three-compartment cell. An Ag/AgCl electrode (Argenthal, 3 M KCl, 0.207 V vs. SHE at 25 °C) was used as the reference and a piece of platinum gauze was employed as the counter electrode. A Luggin capillary was used to minimize errors due to *iR* drop in the electrolytes. All solutions used in this work were prepared with 18 MΩ cm water produced by a reagent water system (Milli-Q SP, Japan).

3. Results and discussion

Typical cyclic voltammograms of graphite measured in 25 mM $VOSO_4$ (denoted as solution 1) and the 25 mM $VOSO_4$ solution with 5 mM H_2O_2 (denoted as solution 2) are shown in Fig. 1 as curves 1 and 2, respectively. The open-circuit potentials of solutions 1 and 2, equal to ca. 0.30 and 0.42 V (vs. Ag/AgCl), respectively, are set as the lower potential limits of CV in Fig. 1. Clearly, there is a pair of redox peaks with their formal potential at ca. 0.6 V on both curves, corresponding to the V^{5+}/V^{4+} transition. However, oxidation of VO^{2+} into V^{5+} (e.g., VO_2^+) does not guarantee successful deposition of vanadium oxide since V^{5+} species have been found to be stable and soluble in aqueous media [19]. Accordingly, a clear reduction peak is visible on the negative sweeps. Since no sensible vanadium oxide is formed on graphite when solution 1 is anodized at 0.7 V for 10 min, most V^{5+} species formed in pure $VOSO_4$ are soluble in solution 1. On the other hand, vanadium oxide is steadily deposited onto graphite from solution 2 at 0.7 V, revealing the enhanced deposition rate of vanadium oxide in the $VOSO_4 + H_2O_2$ solution. This phenomenon indicates that the prior presence of V^{5+} in the precursor solution enhances precipitation of vanadium oxide (converted from the V^{5+} species just being oxidized at the vicinity of substrates). The prior presence of V^{5+} is strongly supported by the decrease in the redox current density on curve 2 in comparison with curve 1. The much lower redox current density on curve 2 results from a lower concentration of VO^{2+} in solution 2, reasonably due to the partial oxidation of VO^{2+} into V^{5+} species by H_2O_2. These V^{5+} species strongly interact with VO^{2+} to form a favorable structure (presuming hydrated VO^{2+}–VO_2^+ complex) for the chemical transformation of V^{5+} (and ca. 11% V^{4+} species) into vanadium oxide when it is oxidized at the substrate vicinity.

Fig. 2 shows the XPS core-level spectra of V $2p_{3/2}$ and O 1s for a vanadium oxide deposit formed at 0.7 V. In Fig. 2A, the XPS spectrum can be decomposed into two peaks centered at 517.1 and 515.6 eV, corresponding to V^{5+} and V^{4+}, respectively [10,12,21,22]. This reveals that the deposit consists of mixed valence compounds containing V^{4+} and V^{5+}. From the relative areas of fitted curves, there are about 11 mol.% V^{4+} species in this oxide. In Fig. 2B, the O 1s spectrum can be decomposed into three constituents (e.g. 529.7, 530.4 and 531.7 eV [10,14,22]) corresponding to V–O–V, V–O–H and H–O–H, respectively. This result reveals the hydrous nature of vanadium oxide deposited from aqueous media. Accordingly, hydrous vanadium oxide prepared in this work is reasonably denoted as $VO_x{\cdot}yH_2O$.

Fig. 3 shows the textural characteristics of a $VO_x{\cdot}yH_2O$ deposit prepared from solution 2. Fig. 3A and B shows the surface morphology of this deposit, revealing a mixed mesoporous–macroporous structure in a 3-D network. There is no obvious grain boundary on this deposit. From Fig. 3C, the cross section image of this deposit shows a porous top layer while a relatively dense layer is formed under this porous layer, supporting the mixed

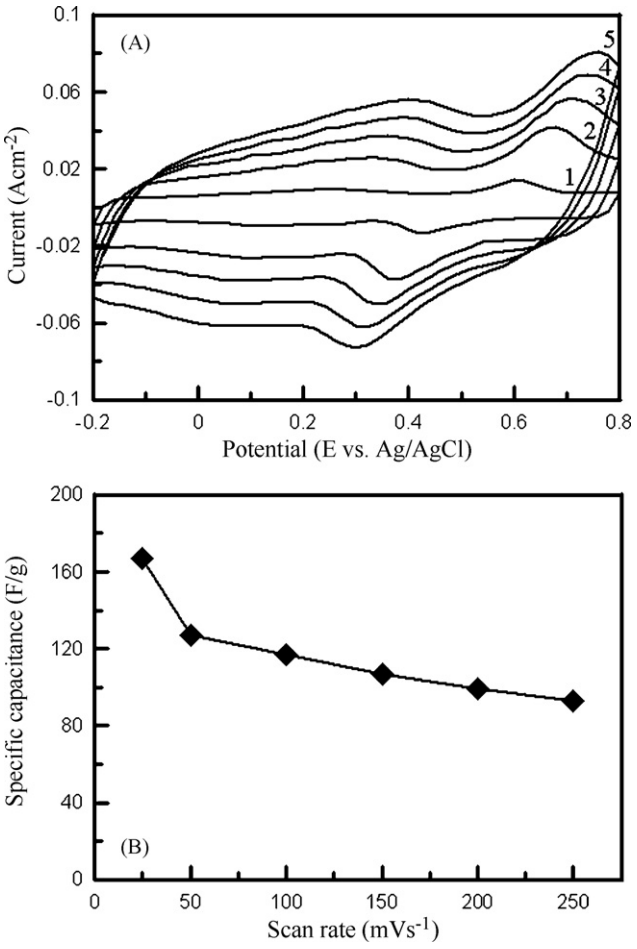

Fig. 4. (A) Cyclic voltammograms measured at (1) 25, (2) 100, (3) 150, (4) 200, and (5) 250 mV s^{-1} and (B) dependence of C_S on the scan rate of CV for a $VO_x{\cdot}yH_2O$ deposit in 3 M KCl.

mesoporous–macroporous structure. The average thickness estimated from the inset of Fig. 3C is about 8.1 μm. The above highly porous, uniform structure is not attributable to anchoring of oxygen bubbles because this deposit was plated at 0.7 V (vs. Ag/AgCl) that is much more negative to oxygen evolution. The diffraction peaks on the XRD pattern in Fig. 3D corresponding to V_2O_5, $V_2O_5{\cdot}1.6H_2O$, and V_6O_{13} reveal a mixture of three crystalline vanadium oxides. The formation of the unique porous structure may be ascribed to the crystalline structures of this deposit (similar to MnO_x deposits found previously [14]) although the exact reason is still unclear. On the other hand, the 3-D porous network architecture is favorable for electrolyte penetration into the whole oxide matrix, which is good for electrochemical energy storage systems, especially high power applications (e.g., ECs).

The novel electrochemical characteristics of $VO_x{\cdot}yH_2O$ with a 3-D porous network structure shown in Fig. 4 are used to demonstrate its promising applicability to ECs in aqueous media. Fig. 4A shows the typical cyclic voltammograms of $VO_x{\cdot}yH_2O$ measured at CV scan rates from 25 to 250 mV s^{-1}. Clearly, there is a pair of redox peaks between 0.3 and 0.7 V on all curves. The similar *i*–E responses at different CV scan rates indicate that all electrochemical reactions on/within the $VO_x{\cdot}yH_2O$ network are highly reversible. To the best of our knowledge, no vanadium oxide shows such *i*–E responses in aqueous KCl solution. In addition, for pure vanadium oxide or composites [11,23,24], capacitive-like behavior under a high scan rate of 250 mV s^{-1} is never found before, especially the oxide loading is about 2 mg cm^{-2} (geometric capacitance >330 mF cm^{-2}). The

specific capacitance of this oxide deposit is equal to ca. 167 F g^{-1} when the scan rate is 25 mV s^{-1}. These novel properties may be linked to the unique porous structure of $VO_x{\cdot}yH_2O$, favoring ion exchange during redox transitions. The specific capacitance of this oxide deposit gradually decreases from ca. 167 to 93 F g^{-1} when scan rates increase from 25 to 250 mV s^{-1} (Fig. 4B), probably due to the formation of a relatively dense layer under the porous top layer. The above capacitive performances reveal that the 3-D networked $VO_x{\cdot}yH_2O$ deposit is a promising candidate of electrode materials for high-power EC applications. Further studies on the deposition mechanism, detailed textural analyses, annealing, and cycling stability, will be performed recently.

4. Conclusions

This work describes the important finding that a new type $VO_x{\cdot}yH_2O$ with a porous 3-D network architecture shows promising pseudocapacitive performances in 3 M KCl (e.g., specific capacitance of ca. 167 F g^{-1} at 25 mV s^{-1} and geometric capacitance of 330 mF cm^{-2}). The capacitive-like behavior of $VO_x{\cdot}yH_2O$ under a high scan rate of 250 mV s^{-1}, never found before, is attributable to its intrinsic porous structure, favoring ion exchange during redox transitions. This unique $VO_x{\cdot}yH_2O$ deposit is plated at a potential much more negative to oxygen evolution (0.7 V vs. Ag/AgCl) from $VOSO_4$ with the prior presence of V^{5+} (25 mM $VOSO_4$ with 5 mM H_2O_2). Through X-ray photoelectron spectroscopic analyses, this oxide deposit, mainly consisting of V^{5+} with 11 mol.% V^{4+}, shows a hydrous nature.

Acknowledgments

The financial support of this work, by the National Science Council of the Republic of China under contract no. NSC 96-2628-E-007-146-MY2, is gratefully acknowledged.

References

[1] E. Shembel, R. Apostolova, V. Nagirny, D. Aurbach, B. Markovsky, J. Power Sources 81–82 (1999) 480.
[2] R. Chen, T. Chirayil, P. Zavalij, M.S. Whittingham, Solid State Ionics 86–88 (1996) 1.
[3] K. West, B. Zachau-Christiansen, T. Jacobsen, S. Skaarup, Electrochim. Acta 38 (1993) 1215.
[4] B. Chaloner-Gill, D.R. Shackle, T.N. Andersen, J. Electrochem. Soc. 147 (2000) 3575.
[5] P.N. Trikalitis, V. Petkov, M.G. Kanatzidis, Chem. Mater. 15 (2003) 3337.
[6] E. Shouji, D.A. Buttry, Langmuir 15 (1999) 669.
[7] W. Dong, D.R. Rolison, B. Dunn, Electrochem. Solid-State Lett. 3 (2000) 457.
[8] T. Kudo, Y. Ikeda, T. Watanabe, M. Hibino, M. Miyayama, H. Abe, K. Kajita, Solid State Ionics 152 (2002) 833.
[9] G.X. Wang, B.L. Zhang, Z.L. Yu, M.Z. Qu, Solid State Ionics 176 (2005) 1169.
[10] C.-C. Hu, K.-H. Chang, Electrochem. Solid-State Lett. 7 (2004) A400.
[11] M. Jayalakshmi, M. Mohan Raoa, N. Venugopal, K.-B. Kim, J. Power Sources 166 (2007) 578.
[12] K.-H. Chang, C.-C. Hu, Acta Mater. 55 (2007) 6192.
[13] J. Livage, Chem. Mater. 3 (1991) 578.
[14] C.-C. Hu, C.-C. Wang, J. Electrochem. Soc. 150 (2003) A1079.
[15] C.-C. Hu, M.-J. Liu, K.-H. Chang, Electrochim. Acta 53 (2008) 2679.
[16] E. Potiron, A. Le Gal La Salle, S. Sarciaux, Y. Piffard, D. Guyomard, J. Power Sources 81–82 (1999) 666.
[17] Y. Sato, H. Yamada, K. Kobayakawa, J. Met. Finish. 39 (1988) 517.
[18] Y. Sato, T. Nomura, H. Tanaka, K. Kobayakawa, J. Electrochem. Soc. 138 (1991) L37.
[19] E. Potiron, A. Le Gal La Salle, A. Verbaere, Y. Piffard, D. Guyomard, Electrochim. Acta 45 (1999) 197.
[20] D.L. da Silva, R.G. Delatorre, G. Pattanaik, G. Zangari, W. Figueiredo, R.-P. Blum, H. Niehus, A.A. Pasa, J. Electrochem. Soc. 155 (2008) E14.
[21] J. Mendialdua, R. Casanova, Y. Barbaux, J. Electron Spectrosc. Relat. Phenom. 71 (1995) 249.
[22] J.F. Moulder, W.F. Stickle, P.E. Sobol, K.D. Bomben, Handbook of X-ray Photoelectron Spectroscopy, Physical Electronics, MN, 1995.
[23] H.Y. Lee, J.B. Goodenough, J. Solid State Chem. 148 (1999) 81.
[24] Z.J. Lao, K. Konstantinov, Y. Tournaire, S.H. Ng, G.X. Wang, H.K. Liu, J. Power Sources 162 (2006) 1451.